ELSEVIER

Biochemical Pharmacology 63 (2002) 1443–1452

Biochemical Pharmacology

Induction of apoptosis in HL-60 leukemia and B16 melanoma cells by the acronycine derivative S23906-1

Jérôme Kluza[a], Amélie Lansiaux[a], Nicole Wattez[a], Marie-Paule Hildebrand[a], Stéphane Léonce[b], Alain Pierré[b], John A. Hickman[b], Christian Bailly[a,*]

[a]*INSERM U-524 et Laboratoire de Pharmacologie Antitumorale du Centre Oscar Lambret, IRCL, Place de Verdun, 59045 Lille, France*

[b]*Institut de Recherches SERVIER, Suresnes, France*

Received 17 September 2001; accepted 13 January 2002

Abstract

The benzoacronycine derivative S23906-1 is a highly potent antitumor agent with a broad spectrum of activity against different human solid tumor xenografts. The marked cytotoxic potential of this drug may be the result of its interaction with DNA but the precise mechanism of action remains unclear at present. We have investigated the induction of apoptosis in human promyelocytic leukemia HL-60 and murine melanoma B16 cells treated with S23906-1. With both cell lines, the drug induces cell cycle perturbations (G2/M arrest) and triggers apoptosis as revealed by the externalization of Annexin V-targeted PS residues at the periphery of the cells. But the biochemical pathways leading to apoptosis are different for the two cancer cell lines. In HL-60 cells, the drug induces significant variations of the $\Delta\Psi_{mt}$, measured by flow cytometry using the fluorochromes JC-1 and cm-X-ros. Activation of caspase-3 and chromatin condensation in HL-60 cells exposed to submicromolar concentrations of S23906-1 for 24 hr were also clearly seen by flow cytometry and confocal microscopy experiments. In contrast, the extent of apoptosis induced by S23906-1 was found to be much more limited in B16 cells. No significant variations of $\Delta\Psi_{mt}$ and no cleavage of the fluorescent caspase-3 substrate GDEVDGI (PhiPhiLux-G_1D_2 probe) could be detected by cytometry in B16 cells exposed to S23906-1. In addition, we characterized the mitochondrial production of reactive oxygen species (ROS) using the probe dihydroethidine (HE) and the variations of the mitochondrial mass using the cardiolipin-interacting probe nonyl acridine orange (NAO). S23906-1 stimulates the production of ROS in both cell lines but the number of mitochondria seems to increase only in drug-treated B16 cells. Collectively these findings identify S23906-1 as a potent inducer of cell apoptosis in the leukemia cells and to a lower extent in the melanoma cells. The results help to understand the downstream cytotoxic actions of this new anticancer agent which is currently undergoing preclinical development.

Keywords: Acronycine; Apoptosis; Cell cycle; Mitochondria; Caspases; Anticancer drug; S23906-1

1. Introduction

Acronycine (Fig. 1) is a cytotoxic alkaloid originally isolated half a century ago from the bark of the Australian scrub ash *Achronychia baueri* [1,2]. While this natural product showed preferential cytotoxicity against certain tumor cells *in vitro*, it had only weak activity *in vivo* [3]. Structure–activity relationship studies have recently led to the development of acronycine derivatives with improved pharmacological properties [4,5]. One of the analogues, S23906-1, bearing two acetate groups at positions 1 and 2 (Fig. 1) has demonstrated promising *in vivo* activity against colon 38 adenocarcinoma implanted in mice [5]. Very recently, highly potent antitumor activities were found against orthotopic models of human solid tumors, including ovarian, lung and colon cancers. S23906-1 was as efficient as paclitaxel, vinorelbine and irinotecan to inhibit the growth of these tumors [6].

The molecular mechanism of action of S23906-1 remains largely unknown. Acronycine inhibits DNA and RNA syntheses and it has been suggested that the alkaloid can intercalate into DNA [7–10]. S23906-1 may also

* Corresponding author. Tel.: +33-320-16-92-18; fax: +33-320-16-92-18-29.

E-mail address: bailly@lille.inserm.fr (C. Bailly).

Abbreviations: LSCM, laser scanning confocal microscopy; cm-X-ros, chloromethyl-X-rosamine; JC-1, tetrachloro-tetraethylbenzimidazol carbocyanine iodide; S23906-1, (+)-*cis*-1,2-diacetoxy-6-methoxy-3,3,14-trimethyl-1,2,3-14-tetrahydro-7*H*-benzo[*b*]pyrano[3,2-*h*]acridin-7-one; $\Delta\Psi_{mt}$, mitochondrial membrane potential.

0006-2952/02/$ – see front matter
PII: S0006-2952(02)00899-7

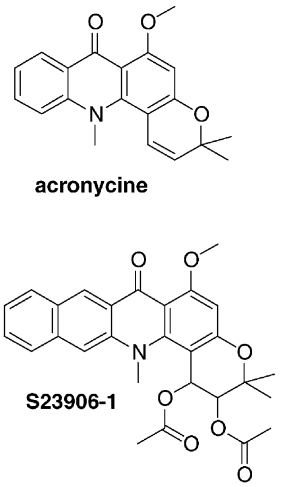

Fig. 1. Structure of acronycine and its synthetic derivative S23906-1.

interact with DNA but however, no published reports assessed the molecular mechanism of action of acronycine derivatives. Also, despite promising *in vivo* activities, the mechanism of cytotoxicity of S23906-1 and related compounds remain unclear at present. It was shown recently that the drug induces cyclin E and inhibits DNA synthesis in HT29 colon carcinoma cells [11]. Our study examined the effects of S23906-1 on the cell cycle progression and the induction of apoptosis. Two cell lines were selected for this study: HL-60 human leukemia cells which are readily prone to enter apoptosis and B16 murine melanoma cells which in general do not easily respond to cytotoxic agents. The goal of the present study was to characterize some of the biochemical and molecular events occurring in various stages leading to cell death induced by S23906-1.

2. Materials and methods

2.1. Drug and chemicals

The synthesis of the benzoacronycine derivative S23906-1 ((±)-*cis*-1,2-diacetoxy-1,2-dihydrobenzoacronycine) has been reported recently [5]. The drug was dissolved in DMSO at 5 mM and then further diluted with water. The DMSO stock solution was kept at −20° and freshly diluted to the desired concentration immediately before use. JC-1 and cm-X-ros (also known as Mitotracker Red™) were from Molecular Probes, Inc. All other chemicals were analytical grade reagents.

2.2. Cell cultures and survival assay

Human HL-60 promyelocytic leukemia cells were obtained from the American Tissue Culture Collection. Cells were grown at 37° in a humidified atmosphere containing 5% CO_2 in RPMI 1640 medium, supplemented with 10% fetal bovine serum, glutamine (2 mM), penicillin (100 IU/mL) and streptomycin (100 μg/mL). B16 melanoma cells were obtained from Dr. M.-C. De Pauw (University of Liège, Belgium). The melanocytes were maintained as monolayers in 150 cm^2 culture flasks using culture medium consisting of DMEM–glutaMAX medium (Gibco) supplemented with 10% fetal bovine serum, penicillin (100 IU/mL) and streptomycin (100 μg/mL). Cells were grown in a humidified atmosphere at 37° under 5% CO_2. B16 cells were harvested by trypsinization and plated 20 hr before treatment with the test drug. A Leica DLMB microscope was used to examine the morphology of adherent cells and counting using a Nageotte cell. In the exponential phase, the doubling time of these melanocytes ranges from 15 to 18 hr and the confluence stage was achieved at a cell density of 3×10^5 cells/cm^2. For the microscopic observations, cells were stained with the standard Pap method [12].

The cytotoxicity of S23906-1 was assessed using a cell proliferation assay developed by Promega (CellTiter 96® AQ_{ueous} one solution cell proliferation assay). Briefly, 2×10^4 exponentially growing cells were seeded in 96-well microculture plates with various drug concentrations in a volume of 100 μL. After 72 hr incubation at 37°, 20 μL of MTS [13] were added to each well and the samples were incubated for a further 3 hr at 37°. Plates were analyzed on a Labsystems Multiskan MS (type 352) reader at 492 nm.

2.3. Cell cycle analysis

A commercial assay, Cycle TEST™ PLUS (Becton-Dickinson), was used for flow cytometry analysis of DNA content. Briefly, 10^6 cells in exponential growth were treated with 0.001–1 μM of S23906-1 for 24 hr and then washed three times with citrate buffer. The cell pellet was incubated with 250 μL of solution A (trypsin-containing citrate buffer) for 10 min at room temperature and then with 200 μL of solution B (citrate buffer containing a trypsin inhibitor and RNase) for 10 min before adding 200 μL of solution C (propidium iodide (PI) at 125 μg/mL and spermin tetrahydrochloride). Samples were analyzed on a Becton Dickinson FACScan flow cytometer using the Cell Quest software (Becton-Dickinson) which is also used to determine the percentage of cells in the different phases of the cell cycle. PI was excited at 488 nm, and fluorescence analyzed at 620 nm (Fl-3).

2.4. Externalization of phosphatidyl serines (PS)

Surface exposure of PS by apoptotic HL-60 and B16 cells was measured by cytometry by adding Annexin V–FITC to 10^6 cells per sample according to the manufacturer's specifications (ApopNexin™ apoptosis detection kit, Oncor®, Appligene). Simultaneously, the cells were stained with PI. Excitation was set at 488 nm and the emission filters used were 515–545 nm (green, FITC)

and 600 nm (red, PI). Data analysis was performed with the standard Cell Quest software.

2.5. Mitochondrial energization

Mitochondrial energization was determined as the retention of fluorescent dyes. After the drug treatment, 10^6 cells in 1 mL of PBS were loaded with the fluorescent probe, either JC-1 (1 μM) or cm-X-ros (25 nM), during 30 min at 37° before the flow cytometric analysis. The same incubation time was applied to the controls and the drug-treated samples. The fluorescence of the dye cm-X-ros was recorded on channel Fl-3. Forward and side scatterings were analysed after linear amplification. With JC-1, both the green (Fl-1) and red (Fl-2) fluorescences were recorded.

2.6. Mitochondrial generation and effects of ROS

After drug treatment, 2×10^6 cells in 5 mL of complete culture medium were collected by centrifugation (10 min, 400 *g*, 4°), washed once with buffer and resuspended in 0.7 mL of PBS before adding the fluorescent probe. HE and NAO were used at 2.5 μM and 100 nM, respectively. In both cases, cells were incubated with the probe for 30 min at room temperature under gentle stirring and then the fluorescence was directly recorded with the cytometer using channels Fl-3 and Fl-1 for HE and NAO, respectively.

2.7. DEVD cleavage activity

To measure caspase activity after drug treatment, the cells were centrifuged, washed with PBS and resuspended in 20 μL of PhiPhiLux-G_1D_2 substrate (OncoImmunin Inc.) for 1 hr at 37° following the manufacturer's protocol. Cleavage of the peptide linker of PhiPhiLux (sequence DEVD) separate the rhodamine moieties and results in fluorescence detectable by flow cytometry.

2.8. Chromatin condensation

B16 cells (20,000 cells/cm^2) were incubated with graded concentrations of S23906-1 at 37° for 24 hr. The medium was removed, the cells were rinsed 10 min with ice-cold PBS and then, fixed with a 2% paraformaldehyde solution for 25 min at +4°. After washing, the cells were incubated with the fluorescent probe Hoechst 33342 (1 μM) for 30 min at 37° in the dark and washed again with PBS. A drop of anti-fade solution was added and the treated portion of the slide was covered with a glass coverslip. The blue fluorescence of the nuclear dye was detected and localized by fluorescence microscopy using a Zeiss microscope with a 63× or 100× oil objective. Images were captured using a software Quips Smart Capture™ (Vysis).

3. Results

3.1. Cytotoxicity and cell cycle effects

A conventional tetrazolium-based assay was used to evaluate the effect of the benzoacronycine derivative S23906-1 on the growth of HL-60 leukemia cells and B16 melanoma cells. In both cases, a dose-dependent inhibition of growth was observed. After 72 hr, the 50% inhibitory concentration of S23906-1 was 0.22 (±0.06) μM and 0.51 (±0.09) μM for HL-60 and B16 cells, respectively. To investigate the effects of S23906-1 on cell cycle progression of HL-60 and B16 cells, the DNA content of cell nuclei was measured by flow cytometric analysis. The cells were treated with graded concentrations of the drug for 24 hr. DNA histograms show that S23906-1 increases the population of G2/M B16 cells in a dose-dependent manner (Fig. 2). The G2/M population increased from 10% in the control to 45% in cells treated with 1 μM S23906-1, while concomitantly the G1 population decreased by half, from 68 to 32%. The percentage of S phase cells was not profoundly affected. With the leukemia cell line, S23906-1 action resulted in a progressive generation of cells having a hypodiploid DNA content (sub-G1 material) that is characteristic of apoptosis and reflects fragmented DNA. Quantitation of the sub-G1 material indicates that this population represents 89% of the cells upon treatment with 1 μM S23906-1. Elevated levels of sub-G1 cells were seen for drug concentrations >0.2 μM, i.e. for doses exceeding the IC_{50} (Fig. 2). For the HL-60 cells, there may be a direct relationship between the doses required to induce programmed cell death and to inhibit cell growth. The appearance of the sub-G1 population is accompanied by characteristic morphological changes. In parallel to the

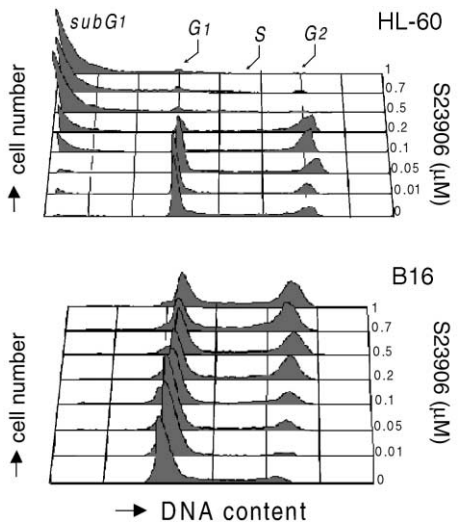

Fig. 2. Cell cycle distribution determined by flow cytometry in HL-60 and B16 cells treated with graded concentration of S23906-1 for 24 hr. Cells were analyzed with the FACScan flow cytometer (Fl-3). Results show a typical experiment which has been repeated three times.

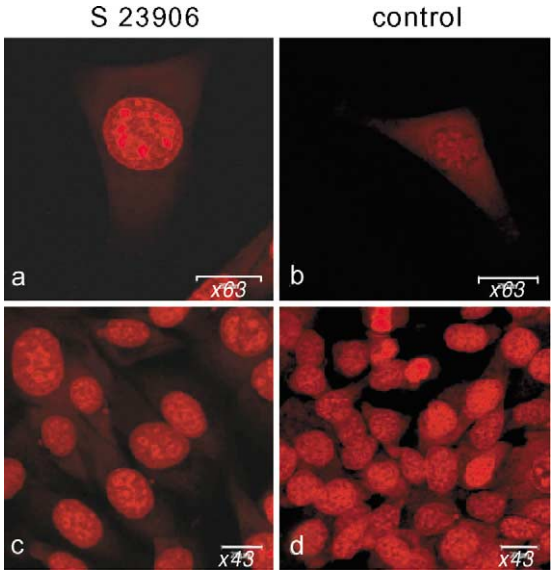

Fig. 3. Fluorescence microscopy images of PI-stained B16 melanoma cells. In panels (a) and (c), cells were treated with 0.5 μM S23906 for 24 hr whereas panels (b) and (d) show untreated control cells. A trypsin-containing solution was used to permeabilize the cells. The magnifications and scales (20 μm) are indicated. The cells shown are representative of the entire population.

cytometry study, the cells loaded with PI were observed under the fluorescence microscope to assess drug-induced changes of the cell morphology. As shown in Fig. 3, the melanocytes treated with S23906-1 were much larger than the control cells. In particular, the size of nuclei, where the red fluorescence of PI accumulates, was considerably increased and the nuclear content stained very strongly. The change in the nuclear texture suggests that S23906-1 affects the chromatin structure and this may indicate that the drug binds directly to DNA. Recent studies at the molecular levels suggest that S23906-1 can alkylate DNA (manuscript in preparation).

3.2. Loss of plasma membrane asymmetry during apoptosis

To further characterize S23906-1-induced apoptosis, we performed a biparametric cytofluorimetric analysis using PI and Annexin V–FITC which stain DNA and PS residues, respectively. Annexin V is a Ca^{2+}-dependent phospholipid binding protein with high affinity for PS. After the drug treatment, the cells were labeled with these two dyes, washed and the resulting red (PI) and green (FITC) fluorescence was monitored by flow cytometry. The results obtained with the HL-60 cell line are displayed in Fig. 4. As indicated on the figure, the percentage of Annexin V positive cells increased gradually upon treatment with S23906-1. At 0.1 μM, 20% of the cells stained positively with Annexin V but practically not with PI (early stage of apoptosis) and at 1 μM the percentage of Annexin V positive cells reached about 80% but at this concentration all cells were also colored in red by PI (late stages of apoptosis and/or dead cells). For similar experiments performed with B16 cells, the percentage of Annexin V positive cells was about 30% at 0.1 μM S23906-1 but in

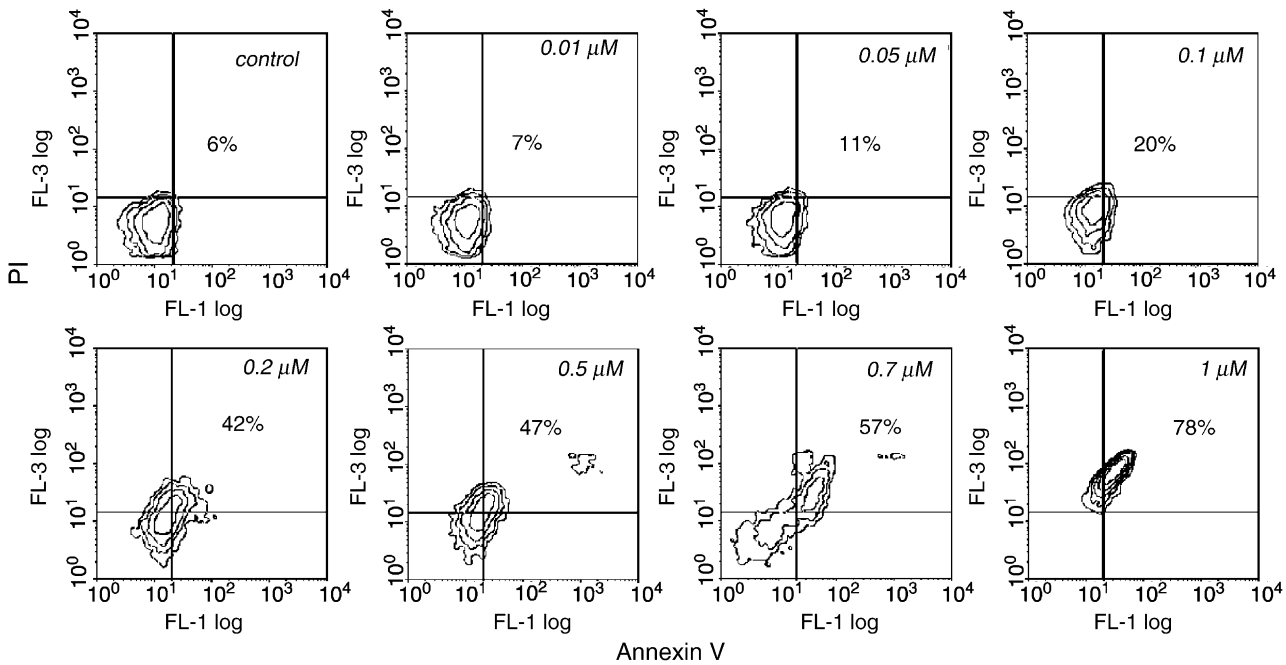

Fig. 4. S23906-1 induces externalization of PS. Contour plots for HL-60 cells treated with graded concentrations of S23906-1 for 24 hr and then stained with PI and an Annexin V–FITC conjugate specifically detecting the exposure of PS residues at the cell surface. Fluorescence intensities (Fl-1 and Fl-3) are shown as log scales. For each drug concentration tested, the percentage of Annexin V^+ cells is given (±3%). Results show a typical experiment which has been repeated four times.

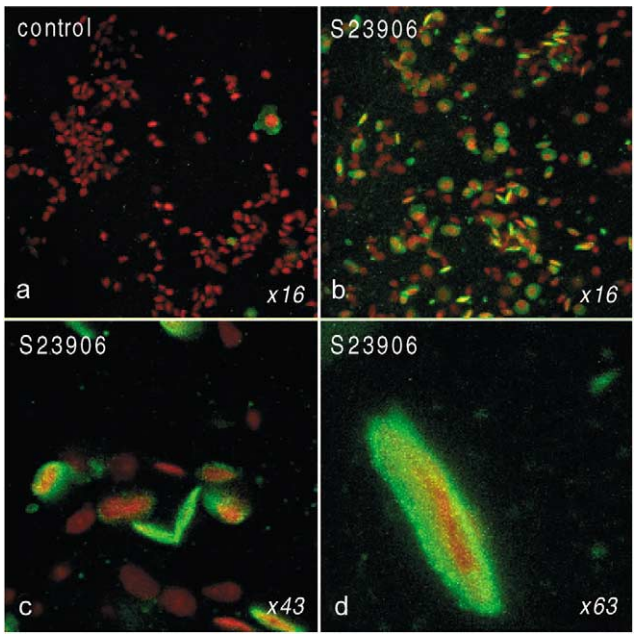

Fig. 5. Annexin V binding to B16 cells treated with S23906-1. (a) Control cells (magnification: 16×); (b–d) cells treated with S23906-1 at 0.5 μM for 24 hr (magnification: 16×, 43×, 63×). PS residues exposed at the surface of the cells bind to Annexin V–FITC conjugate thus providing a green fluorescence at the cell periphery. At the same time, cells were stained with PI to stain the nuclei, before examination under a confocal laser-scanning microscope. The magnifications are indicated. The experiment was performed three times with identical results.

this case, the flow cytometry analysis is less appropriate because membrane damage can occur during harvesting. In addition, harvesting with trypsin and EDTA can also influence the measurable amount of bound Annexin V, because trypsin and EDTA remove bound Annexin V from the surface by proteolysis and chelation of Ca^{2+}, respectively. For these reasons, we evaluated the number of Annexin V positive B16 cells by means of fluorescence microscopy without their detachment from the glass slides directly incubated in the culture flasks. Typical images are shown in Fig. 5. The control cells showed no green fluorescence whereas about 35% of the cells treated with 0.5 μM S23906-1 for 24 hr were colored in green. The FITC fluorescence can easily be localized at the periphery of the cells reflecting the translocation of PS residues from the inner leaflet of the plasma membrane to the outer leaflet. PS exposed to the external environment are thus directly accessible to Annexin V–FITC. These data indicate that S23906-1 provokes the loss of membrane asymmetry in both cell lines.

3.3. Variations of the $\Delta\Psi_{mt}$

$\Delta\Psi_{mt}$ was monitored by fluorescence of the dye JC-1 which is considered a reliable probe to assess $\Delta\Psi_{mt}$ changes [14]. JC-1 has the unique property of forming red-fluorescent J-aggregates locally and spontaneously under high mitochondrial $\Delta\Psi_{mt}$ whereas the monomeric

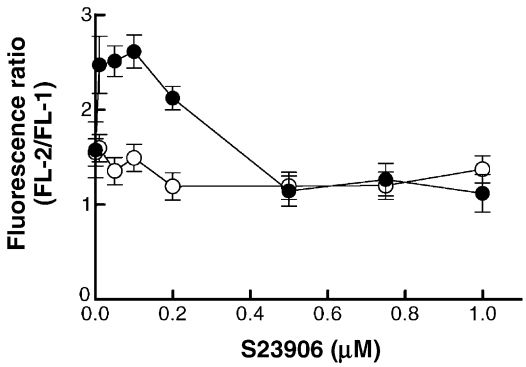

Fig. 6. Variations of the red/green (Fl-2/Fl-1) fluorescence ratio as a function of the S23906-1 concentration. (●) HL-60 and (○) B16 cells were treated with graded concentrations of S23906-1 for 24 hr before staining with the probe JC-1. The green fluorescence refers to the JC-1 monomers and the red fluorescence corresponds to the formation of J-aggregates. Mean ± SD of three independent experiments.

form fluoresces green [15]. Cells were treated with increasing concentrations of S23906-1 for 24 hr before labeling with 1 μM JC-1. The changes of the ratio of red/green fluorescence reflect the variations of $\Delta\Psi_{mt}$ independently of the mitochondrial mass. Untreated cells exhibit at the same time intensive green and red fluorescence. Fig. 6 shows the variations of the fluorescence ratio Fl-2/Fl-1 (red/green fluorescence) as a function of the drug concentration. Almost no effect was observed with B16 cells. In contrast, with HL-60 cells, low drug concentrations induce an increase of the fluorescence ratio followed by a decrease at higher concentrations.

Similar experiments were performed with the dye cm-X-ros which is sensitive to the mitochondrial mass, unlike JC-1. Here again, the detection of mitochondrial polarization using cm-X-ros was also accomplished by cytometry and the results are presented in Fig. 7. Treatment of the HL-60 cells with 0.2 μM S23906-1 induces a marked increase of the cm-X-ros fluorescence. At 0.5 μM, the hyperpolarization peak decreases and a second peak corresponding to a much lower fluorescence appeared. The decrease of the fluorescence intensity reflects the drug-induced depolarization of the inner mitochondrial membrane. The dissipation of $\Delta\Psi_{mt}$ reflects the opening of the mitochondrial permeability transition pores. This effect, which has been commonly observed with other anticancer drugs irrespective of the cell type, generally defines early but already irreversible stage of apoptosis. With B16 cells, we could only detect an increase of the cm-X-ros fluorescence. Because no such effect was seen with the probe JC-1, we suspected that this unusual effect arises from a drug-induced increase of the mitochondrial mass rather than an increase of $\Delta\Psi_{mt}$. As mentioned above, cm-X-ros but not JC-1 is sensitive to the mitochondrial mass. Direct examination of the B16 cells under the confocal microscope support this hypothesis. As shown in Fig. 8, untreated cells demonstrated a punctated pink pattern for cm-X-ros consistent with its mitochondrial localization. Upon treatment

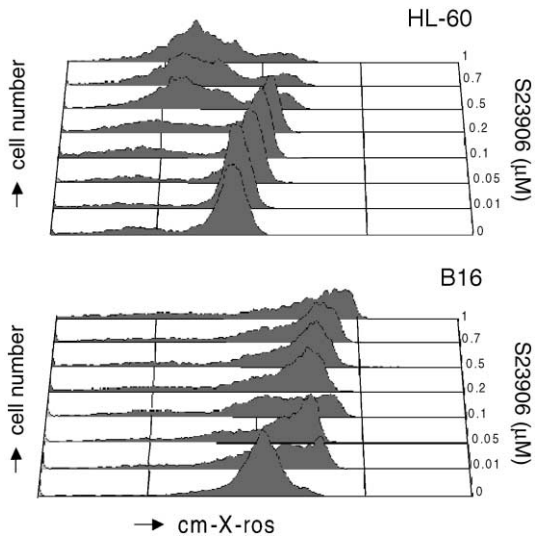

Fig. 7. Variations of the $\Delta\Psi_{mt}$ measured with the dye mitotracker red (cm-X-ros) in HL-60 and B16 cells treated with S23906-1. The cytofluorometric profiles show the variations of the cm-X-ros fluorescence following exposure of the cells to graded concentrations of S23906-1 (0.01–1 μM) for 24 hr. Cells were stained with 25 nM cm-X-ros before analysis by flow cytometry (Fl-3). The experiment was performed three times with identical results.

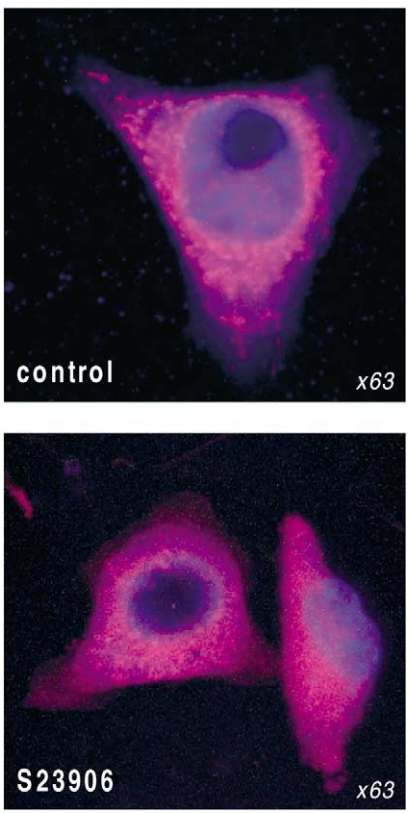

Fig. 8. Fluorescence microscopy images of B16 control cells and cells treated with 0.05 μM S23906-1. After the drug treatment, these cells were processed for mitochondria labeling using the $\Delta\Psi_{mt}$-sensitive dye cm-X-ros (pink). At the same time, cells were stained with the nuclear specific TOTO-3 dye (blue) before examination under a confocal laser scanning microscope. The figure shows typical cells recorded by a blinded observer.

with 0.05 μM S23906-1, a brighter punctate staining was seen throughout the live cells.

3.4. Mitochondrial generation and effects of ROS

We utilized the fluorescent indicator HE, in which fluorescence appears if ROS are generated, to investigate the effect of S23906-1 on the production of oxygen species during apoptosis. HE is oxidized by superoxide anion into ethidium bromide which emits red fluorescence [16]. Superoxide is produced by mitochondria due to a shift from the normal 4-electron reduction of O_2 to a 1-electron reduction when cytochrome *c* is released from mitochondria [17]. The results presented in Fig. 9 indicate that the production of ROS in B16 cells is not significantly changed in the presence of S23906-1 whereas important variations are observed with HL-60 cells. Upon treatment with 0.2–1.0 μM S23906-1 for 24 hr, two cell populations can be distinguished: one with a reduced level of ROS species and one corresponding to an enhanced HE–ethidium conversion consistent with the appearance of an oxidative stress induced by the drug. ROS and the resulting redox change must be part of the transduction pathway during apoptosis induced by S23906-1 in the leukemia cell line.

In parallel, we evaluated the damage produced by ROS in mitochondria by assessing the oxidation state of cardiolipin, a molecule restricted to the inner mitochondrial membrane. The fluorescent probe NAO interacts stoichiometrically with intact, non-oxidized cardiolipin [18]. With B16 cells treated with S23906-1, even at a low concentration of 0.01 μM, a marked increases in NAO fluorescence was observed (Fig. 10) suggesting an increase of the

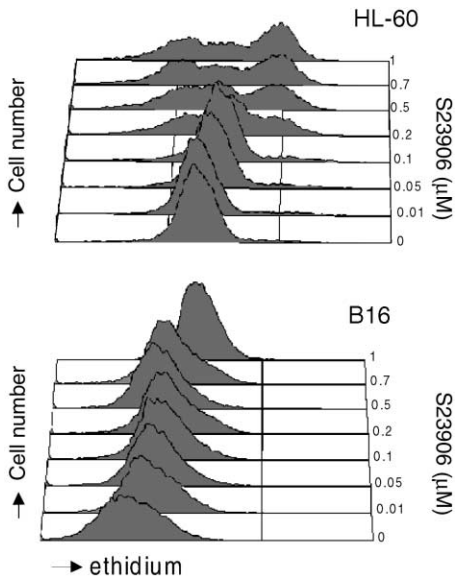

Fig. 9. Modification of ROS production in HL-60 and B16 cells treated with S23906-1. Cells were exposed to graded concentrations of S23906-1 (0.01–1 μM) for 24 hr before the addition of 2.5 μM HE for 30 min. Cells were analyzed with the FACScan flow cytometer (Fl-3). The experiment was performed three times with identical results.

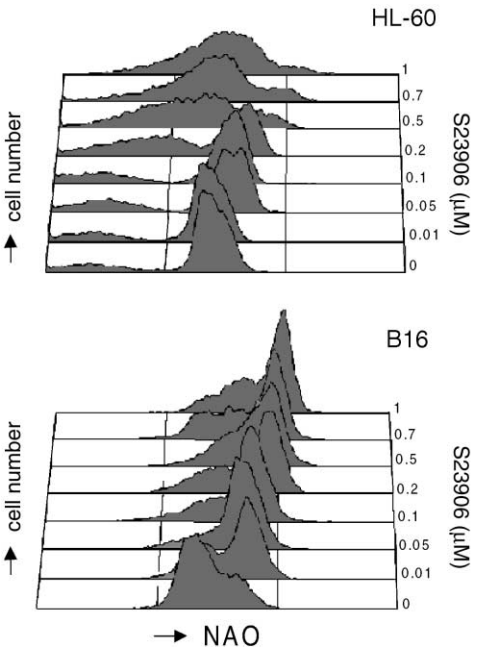

Fig. 10. Effects of S23906-1 on ROS-mediated oxidation of cardiolipins. Cells were exposed to graded concentrations of S23906-1 (0.01–1 μM) for 24 hr before the addition of 100 nM NAO for 30 min. Cells were analyzed with the FACScan flow cytometer (Fl-1). Results are representative of three independent staining.

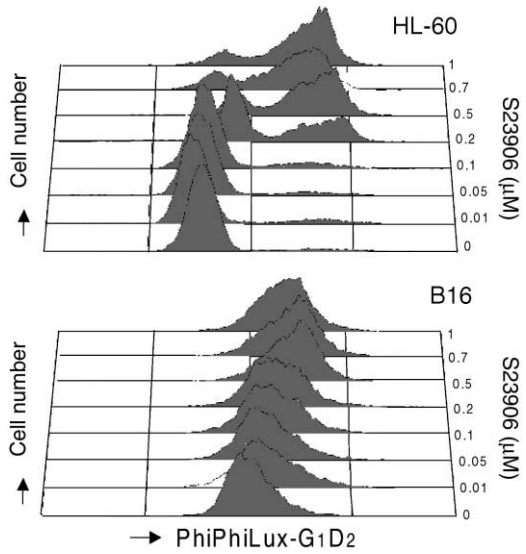

Fig. 11. Drug-induced activation of caspase-3 in HL-60 and B16 cells. Cells were exposed to graded concentrations of S23906-1 (0.01–1 μM) for 24 hr before the addition of the PhiPhiLux-G_1D_2 probe containing a rhodamine-tagged GDEVDGI peptide motif substrate for caspase-3. Cells were analyzed with the FACScan flow cytometer (Fl-1). Data are from a representative experiment.

cardiolipin content as a result of an enhancement of the mitochondrial mass. On the contrary, in HL-60 cells the NAO fluorescence was slightly increased with S23906-1 concentrations <0.2 μM and then for higher concentrations, a cell population characterized by a low NAO fluorescence appeared (Fig. 10). Such a reduction in NAO fluorescence indicates a decrease in cardiolipin content in HL-60 cells treated with 0.2–1.0 μM S23906-1.

3.5. Caspase activation

Many studies have implicated cysteine proteases (caspases) as key participants in the sequence of events that results in the dismantling of the cell during apoptosis [19,20]. Therefore, it was interesting to evaluate the effect of S23906-1 on the activity of caspase-3, one of the major effector caspases. We explored the proteolytic cleavage of the rhodamine-tagged substrate which contains a heptapeptide GDEVDGI recognition sequence for caspase-3 and possibly for other caspases such as caspase-7. As shown in Fig. 11, HL-60 cells treated with S23906-1 showed a massive activation of caspases whereas little cleavage of the rhodamine-based substrate carrying the DEVD peptide backbone was detected in B16 cells.

3.6. Apoptosis in B16 cells treated with S23906-1

The above experiments indicate very clearly that S23906-1 induces apoptosis in HL-60 cells but in contrast the evidences for apoptosis in the B16 cells are much weaker. These melanoma cells are notoriously resistant to most chemotherapeutic agents. Additional experiments were performed to support the idea that S23906-1 also induces apoptosis in B16 cells. Microscopic examination of these cells showed alterations of the nuclear and cytoplasmic membrane morphology induced by S23906-1 (Fig. 12A). With the Papanicolaou staining procedure, the morphology of non-apoptotic cells can be distinguished from that of B16 cells undergoing apoptosis. Non-apoptotic cells are usually rather round and their nucleus is large whereas B16 cells treated with S23906-1 are convoluted and budding, and they frequently present several clumps of condensed chromatin. The identification of apoptotic body-like structures suggest that these cells are effectively engaged in the apoptotic pathway. Nuclei of B16 cells treated with S23906-1 showed a more condensed chromatin than that of untreated control cells, as judged from staining with the blue dye Hoechst 33342 (Fig. 12B) and in agreement with the data in Fig. 3. In parallel, a noticeable fragmentation of the genomic material was detected by a TUNEL assay (TdT-mediated dUTP Nick End Labeling) (data not shown) but the DNA extracted from S23906-1-treated B16 cells showed no internucleosomal DNA cleavage (no ladder). Extensive DNA cleavage was detected neither with S23906-1, nor with other cytotoxic agents like camptothecin or etoposide. Similarly, the PARP protein remained intact in the melanoma cells upon treatment with these different drugs (data not shown). The fragmentation of the genome of these B16 cells seems to produce only high molecular weight DNA fragments. Nevertheless, altogether these data are sufficient to conclude that S23906-1 induces apoptosis of the B16 cells even if these

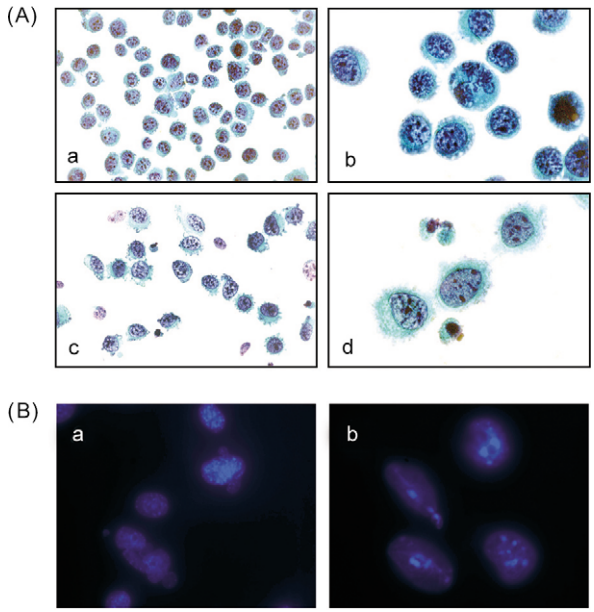

Fig. 12. Changes in morphology of the B16 cells upon treatment with S23906-1. The cells were treated with 5 μM S23906-1 for 24 hr before staining (A) according to the Papanicolaou procedure or (B) with the Hoechst 33342 blue dye. In (A), panels (a) and (b) refer to the control cells with intact morphological features and panels (c) and (d) refer to drug-treated cells with apoptotic characteristics; magnification: (a) and (c) 40×; (b) and (d) 100×. In (B), panel (a) refers to untreated control cells and panel (b) corresponds to the drug-treated cells with a more condensed chromatin; magnification: 63× for (a) and (b).

melanoma cells respond relatively poorly to the apoptotic stimulus.

4. Discussion

The two cell lines used in this study responded quite differently to the treatment with the antitumor agent S23906-1. Treatment of promyelocytic HL-60 cells with the benzoacronycine derivative caused massive death by apoptosis, as determined by the characteristic cell cycle changes (appearance of the sub-G1 population) and the loss of membrane asymmetry (Annexin V positivity). At the same time, important changes of the $\Delta\Psi_{mt}$ and production of ROS were detected by cytometry using specific fluorescent probes. ROS are important regulators of apoptosis [21]. A number of apoptotic stimuli, such as treatment with etoposide and ceramide have been shown to activate ROS generation by mitochondria [22]. These ROS may arise from the pre-apoptotic accumulation of intracellular H_2O_2 [23]. The disruption of the mitochondrial transmembrane potential observed upon treatment of HL-60 cells with S23906-1 is accompanied by the cleavage of the DEVD-containing substrate of certain caspases, in particular caspases-3 and -7. The data clearly indicate that S23906-1 induces apoptosis of HL-60 cells by a caspase-dependent pathway.

With the B16 melanoma cells, the drug S23906-1 also induces apoptosis, as judged from the externalization of PS residues in plasma membrane, but the biochemical events are quite distinct from those seen with the S23906-1-challenged HL-60 cells. In particular with the B16 cells, the drug S23906-1 does not cause a dissipation of the $\Delta\Psi_{mt}$ and no activation of caspase-3 type activity was detected. In contrast, the cytometry data obtained with the fluorescent probes cm-X-ros and NAO were consistent with a drug-induced increase of the mitochondrial mass. It is well established that commitment to apoptosis can involve important changes in mitochondrial activity and mass [24]. It is worth mentioning that in parallel to the cytometry measurements, we also investigated the effect of S23906-1 on the expression of the anti-apoptotic Bcl-2 protein which acts at the mitochondrial level to prevent the release of apoptotic factors (e.g. cytochrome *c* and AIF) and activation of caspases [25]. Bcl-2 expression was analyzed by Western blot (using a monoclonal antibody from Immunotech) but no difference was found between S23906-1-treated and control cells (data not shown). The induction of apoptosis by S23906-1 may be independent of the modulation of expression of Bcl-2, as it is the case with other chemotherapeutic agents [26]. Bcl-2 levels do not generally change after cytotoxins.

Two cationic fluorescent probes, JC-1 and cm-X-ros, have been used to measure the changes of $\Delta\Psi_{mt}$ in response to the treatment of cells with S23906-1. With HL-60 cells, the results are mutually consistent and concur that S23906-1 induces dose-dependent alterations in $\Delta\Psi_{mt}$. A loss of the $\Delta\Psi_{mt}$ is observed upon treatment of HL-60 cells with 0.5 μM concentrations of S23906-1. In sharp contrast, a marked increase in $\Delta\Psi_{mt}$ was detected when the cells were treated with a lower drug concentration of 0.2 μM. The hyperpolarization effect of S23906-1 can result from different actions such as an increased mitochondrial mass and number per cell [27] or to an increases in matrix volume [28]. The disruption of $\Delta\Psi_{mt}$ is associated with the appearance of the sub-G1 cell fraction characteristic of apoptotic cells as judged from the Annexin V positivity. In contrast, the initial increase of $\Delta\Psi_{mt}$ in HL-60 cells is correlated with the arrest of the cell in the G2/M phase of the cell cycle. The subsequent decrease of $\Delta\Psi_{mt}$ coincides with the decrease of the G2 population and appearance of the hypo-diploid DNA content peak. We have recently reported a similar correlation between the cell cycle changes and the $\Delta\Psi_{mt}$ variations in HL-60 cells using the antitumor agents TAS-103 and etoposide [29,30]. At a low dose, these two drug provoke a G2/M cell cycle arrest associated with an increased membrane potential. At a high dose, they stimulate the apoptotic cell death machinery and this was associated with a decline in mitochondrial potential. The dissipation of $\Delta\Psi_{mt}$ is observed concomitantly with the activation of caspase-3 (DEVDase activity) but these two events are not necessarily connected. It has been reported recently that during camptothecin-induced apoptosis of HL-60 cells, caspases are activated independently of the collapse of

$\Delta\Psi_{mt}$ [31]. The variations of $\Delta\Psi_{mt}$ are correlated with the cell cycle changes and they may also be connected with the variations of the mitochondrial cytochrome *c* levels. Indeed, Sanchez-Alcazar *et al*. [32] recently described two phases during camptothecin-induced apoptosis in Jurkat cells: a pre-apoptotic phase characterized by an increase in cytochrome *c* associated with a transient elevation of $\Delta\Psi_{mt}$ and an apoptotic progression phase during which cytochrome *c* is released into the cytosol, associated with the disruption of $\Delta\Psi_{mt}$. Studies are in progress to evaluate further the possible relationships between the hyper- and depolarization of the mitochondrial membrane and the fluctuations of the mitochondrial protein levels.

The apoptosis pathway induced by the drug S23906-1 proceedes differently in HL-60 leukemia cells compared to B16 melanoma cells. At present, it is difficult to conclude whether the observed biochemical pathways reflect the inherent mode of death of the cells or the specific action of S23906-1. But, based on the literature data, the second hypothesis seems more likely. The accumulation of B16 cells in the G2/M phase is commonly observed with many types of cytotoxic agents including the DNA-binding topoisomerase II inhibitor doxorubucin [33], nitrosoureas [34], and the tubulin binding agent A-105972 [35] but this effect is often correlated with an activation of caspases. For example, the anticancer drugs cytostatin and bactobolin [36] can activate caspase-3 in B16 cells. Similarly, caspase-3 is activated during apoptosis induced by the dihydrochalcone phloretin in both B16 and HL-60 cells [37]. On the contrary, we show here that S23906-1 does not activate caspase-3 (Fig. 11) and for this reason, we conclude that this observation must reflect the drug effect more than the inherent property of the B16 cells. An interesting parallel can be established with the *in vivo* activity. S23906-1 is active against a number of tumor models including leukemia but not against B16 melanoma [6]. The lower sensitivity of this cell type to S23906-1-induced apoptosis may explain, at least partially, the lack of antitumor effect observed in the *in vivo* model.

In conclusion, this study identifies the benzoacronycine derivative S23906-1 as a potent inducer of apoptosis in human promyelocytic HL-60 cells and to a lower extent in murine B16 melanoma cells. With the human cell line, the apoptotic death is associated with important changes of the mitochondrial functions such as dissipation of the transmembrane potential and generation of ROS, as well as with a massive activation of caspases. In contrast, the response of the B16 cell line to the treatment with S23906-1 involves a significant increase of the mitochondrial mass with no detectable alteration of the mitochondrial electrochemical potential and no elevated generation of reactive oxygen species. This study confirms that apoptosis, which is a carefully regulated process of cell death, can proceed through different mechanisms according to cell type with a drug like S23906-1. This novel anticancer agent is currently undergoing preclinical development.

Acknowledgments

This work was done under the support of research grants (to C.B.) from the Association pour la Recherche sur le Cancer. The authors thank the *Service Commun d'Imagerie Cellulaire de l'IFR22* for access to the confocal microscope and Christine Bal and Michael Facompré for the maintenance of the cell cultures. We also thank E. Canet and G. Atassi for supporting this collaboration and S. Michel and M. Koch for the synthesis of S23906-1.

References

[1] Hughes GK, Lahey FN, Price JR, Webb LJ. Alkaloids of the Australian rutanaceae. Nature 1948;162:223–4.
[2] Svoboda G, Poore GA, Simpson PJ, Boder GB. Alkaloids of Acronychia Baueri Schott I. Isolation of the alkaloids and a study of the antitumor and other biological properties of acronycine. J Pharm Sci 1966;55:759–68.
[3] Dorr RT, Liddil JD, Von Hoff DD, Soble M, Osborne CK. Antitumor activity and murine pharmacokinetics of parenteral acronycine. Cancer Res 1989;49:340–4.
[4] Elomri A, Mitaku S, Michel S, Skaltsounis AL, Tillequin F, Koch M, Pierré A, Guilbaud N, Léonce S, Kraus-Berthier L, Rolland Y, Atassi G. Synthesis and cytotoxic and antitumor activity of esters in the 1,2-dihydroxy-1,2-dihydroacronycine series. J Med Chem 1996;39:4762–6.
[5] Costes N, Le Deit H, Michel S, Tillequin F, Koch M, Pfeiffer B, Renard P, Léonce S, Guilbaud N, Kraus-Berthier L, Atassi G, Pierré A. Synthesis and cytotoxic and antitumor activity of benzo[b]pyrano[3,2-h]acridin-7-one analogues of acronycine. J Med Chem 2000; 43:2395–402.
[6] Guilbaud N, Kraus-Berthier L, Meyer-Losic F, Malivet V, Chacun C, Jan M, Tillequin F, Koch M, Pfeiffer B, Atassi G, Hickman J, Pierré A. Marked antitumor activity of a new potent acronycine derivative in orthotopic models of human solid tumors. Clin Cancer Res 2001; 7:2573–80.
[7] Gout PW, Dunn BP, Beer CT. Effects of acronycine on nucleic acid synthesis and population growth in mammalian tumor cell cultures. J Cell Physiol 1971;78:127–38.
[8] Dunn BP, Gout PW, Beer CT. Effects of the antineoplastic alkaloid acronycine on nucleoside uptake and incorporation into nucleic acids by cultured L5178Y cells. Cancer Res 1973;33:2310–9.
[9] Reddy SB, Linden WA, Zywietz F, Baisch H, Struck U. Effects of acronycine, bleomycin and cytosine arabinoside on the cell cycle. Arzneim-Forsch/Drug Res 1977;27:1549–53.
[10] Shieh H-L, Pezzuto JM, Cordell GA. Evaluation of the cytotoxic mechanisms mediated by the broad-spectrum antitumor alkaloid acronycine and selected semisynthetic derivatives. Chem-Biol Interactions 1992;81:35–55.
[11] Léonce S, Perez V, Lambel S, Peyroulan D, Tillequin F, Michel S, Koch M, Pfeiffer B, Atassi G, Hickman JA, Pierré A. Induction of cyclin E and inhibition of DNA synthesis by the novel acronycine derivative S23906-1 precede the irreversible arrest of tumor cells. Mol Pharmacol 2001;60:1383–91.
[12] Papanicolaou GN. A new procedure for staining vaginal smears. Science 1942;95:438–9.
[13] Cory AH, Owen TC, Barltrop JA, Cory JG. Use of an aqueous soluble tetrazolium/formazan assay for cell growth assays. Cancer Commun 1991;3:207–12.
[14] Salvioli S, Ardizzoni A, Franceschi C, Cossarizza A. JC-1, but not DiOC6(3) or rhodamine 123, is a reliable fluorescent probe to assess $\Delta\Psi$ changes in intact cells: implications for studies on mitochondrial functionality during apoptosis. FEBS Lett 1997;411:77–82.

[15] Smiley ST, Reers M, Mottolahartshorn C, Lin M, Chen A, Smith TW, Steele GD, Chen LB. Intracellular heterogeneity in mitochondrial membrane potentials revealed by a J-aggregate forming lipophilic cation. Proc Natl Acad Sci USA 1991;88:3671–5.
[16] Rothe G, Valet G. Flow cytometric analysis of respiratory burst activity in phagocytes with hydroethidine and 2′,7′-dichlorofluorescin. J Leukoc Biol 1990;47:440–8.
[17] Nose K. Role of reactive oxygen species in the regulation of physiological functions. Biol Pharm Bull 2000;23:897–903.
[18] Petit JM, Maftah A, Ratinaud MH, Julien R. 10N-nonyl acridine orange interacts with cardiolipin and allows the quantification of this phospholipid in isolated mitochondria. Eur J Biochem 1992; 209:267–73.
[19] Nuñez G, Benedict M, Hu Y, Inohara N. Caspases: the proteases of the apoptotic pathway. Oncogene 1998;17:3237–45.
[20] Earnshaw WC, Martins LM, Kaufmann SH. Mammalian caspases: Structure, activation, substrates, and functions during apoptosis. Annu Rev Biochem 1999;68:383–424.
[21] Suzuki YS, Forman HJ, Sevanian A. Oxidants as stimulators of signal transduction. Free Radical Biol Med 1997;22:269–85.
[22] Garcia-Ruiz C, Colell A, Mari M, Morales A, Fernandez-Checa JC. Direct effect of ceramide on the mitochondrial electron transport chain leads to generation of reactive oxygen species. Role of mitochondrial glutathione. J Biol Chem 1997;272:11369–77.
[23] Galan A, Garcia-Bermejo L, Vilaboa NE, de Blas E, Aller P. Uncoupling of apoptosis and Jun/AP-1 activity in human promonocytic cells treated with DNA-damaging and stress-inducing agents. Eur J Cell Biol 2000;79:1–9.
[24] Vayssiere JL, Petit PX, Risler Y, Mignotte B. Commitment to apoptosis is associated with changes in mitochondrial biogenesis and activity in cell lines conditionally immortalized with simian virus 40. Proc Natl Acad Sci USA 1994;91:11752–6.
[25] Antonsson B, Martinou JC. The Bcl-2 protein family. Exp Cell Res 2000;256:50–7.
[26] Achenbach TV, Muller R, Slater EP. Bcl-2 independence of flavopiridol-induced apoptosis. Mitochondrial depolarization in the absence of cytochrome c release. J Biol Chem 2000;13:32089–97.
[27] Darzynkiewicz Z, Staiano-Coico L, Melamed M. Increase mitochondrial uptake of rhodamine 123 during lymphocyte stimulation. Proc Natl Acad Sci USA 1981;78:2383–7.
[28] Reed JC, Jurgensmeier JM, Matsuyama S. Bcl-2 family proteins and mitochondria. Biochim Biophys Acta 1998;1366:127–37.
[29] Kluza J, Lansiaux A, Wattez N, Mahieu C, Osheroff N, Bailly C. Apoptotic response of HL-60 human leukemia cells to the antitumor drug TAS-103. Cancer Res 2000;60:4077–84.
[30] Facompré M, Wattez N, Kluza J, Lansiaux A, Bailly C. Relationship between cell cycle changes and variations of the mitochondrial membrane potential induced by etoposide. Mol Cell Biol Res Commun 2000;4:37–42.
[31] Li X, Du L, Darzynkiewicz Z. During apoptosis of HL-60 and U-937 cells caspases are activated independently of dissipation of mitochondrial electrochemical potential. Exp Cell Res 2000;15: 290–7.
[32] Sanchez-Alcazar JA, Ault JG, Khodjakov A, Schneider E. Increased mitochondrial cytochrome c levels and mitochondrial hyperpolarization precede camptothecin-induced apoptosis in Jurkat cells. Cell Death Differ 2000;7:1090–100.
[33] Supino R, Mariani M, Colombo A, Prosperi E, Croce AC, Bottiroli G. Comparative studies on the effects of doxorubicin and differentiation inducing agents on B16 melanoma cells. Eur J Cancer 1992; 28A:778–83.
[34] Buchdahl C, Papon J, Communal Y, Bourges M, Madelmont JC. G2 accumulation and melanin overproduction in malignant melanocytes treated with a new nitrosourea. Melanoma Res 1998;8:517–27.
[35] Wu-Wong JR, Alder JD, Alder L, Burns DJ, Han EK, Credo B, Tahir SK, Dayton BD, Ewing PJ, Chiou WJ. Identification and characterization of A-105972, an antineoplastic agent. Cancer Res 2001;61: 1486–92.
[36] Kawada M, Amemiya M, Ishizuka M, Takeuchi T. Differential induction of apoptosis in B16 melanoma and EL-4 lymphoma cells by cytostatin and bactobolin. Jpn J Cancer Res 1999;90:219–25.
[37] Kobori M, Iwashita K, Shinmoto H, Tsushida T. Phloretin-induced apoptosis in B16 melanoma 4A5 cells and HL60 human leukemia cells. Biosci Biotechnol Biochem 1999;63:719–25.